Journal of Theoretical and Applied Information Technology
30th April 2021. Vol.99. No 8

ISSN: 1992-8645 www.jatit.org E-ISSN: 1817-3195

MONITORING THE BREATHING RATE IN THE HUMAN THERMAL IMAGE BASED ON DETECTING THE REGION OF INTEREST

FARAH Q. AL-KHALIDI [1], SHAIMAA H. AL-KANANEE[2], SAMIRA A. A HUSSAIN[3]

[1,3] Department of Computer, College of Science, Mustansiriyah university, Baghdad, Iraq
[2] Department of Computer, College of Science, Technology University, Baghdad, Iraq

Email: [1] farahqaa@uomustansiriyah.edu.iq , [2]120011@uotechnology.edu.iq,
[3]samira.hussain1212@gmail.com

ABSTRACT

Methodology to monitor the breathing rate based on the thermal image processing techniques has been investigated. This approach is based on detecting the skin temperature change of the region. A methodology to monitor the breathing rate based on the thermal image processing techniques has been investigated. This approach is based on detecting skin temperature change of the area of importance (ROI) which represented the range between the tip of the nose and the superior lip of the mouth due to the breathing operation.

The major steps to compute breathing rate included enhancement the thermal imaging to improve the contrast quality and to reduce the noise, Segmenting the region of interest (ROI) from the rest of the image, Applying feature extraction to extract the respiration signal, and then determine respiration rate from the respiration signal. In this study, the manual segmented method to detect the ROI with the alignment technique was investigated.

It was demonstrated that the methods could successfully track the ROI for both regular and random head movement types and could determine respiration rate in a non-contact manner.

The correlation technique was used to measure the accuracy between the reference and the alignment images. Also, three methods were suggested to segment the ROI automatically from the subject's head. The ROI signifies the facial exaggerated part most influenced by inhaled air temperature variations. Further work is in progress to enhance the algorithms so that they can cope with very large head movements.

Keywords: *Thermal Imaging, Region Of Interest, Skin Temperature Change, And Respiration Rate*

1. INTRODUCTION

Monitoring breathing rate is an essential task in clinical diagnosis. Instruments exist to accurately monitor temperature, heart rate, blood pressure, etc. However, currently, there are deficiencies in measuring the breathing rate. Monitoring the respiratory rate in infants poses a challenge as existing techniques have significant limitations. One approach to monitoring respiratory rate is based on attaching electrodes to the patient to record the electrocardiogram, (ECG). The breathing rate is then extracted from the ECG[1]. Werthammer et al., (1983) suggested another invasive method to detect apnea in infants by an acoustic monitor. It depends on the recording of a signal derived from breathing sounds from the nose. This method was used with eight premature infants. The acoustic monitor detects breathing sounds through a microphone [8].

Although this method can detect the absence of airflow during obstructed respiratory efforts or body movements, it also an inaccurate method of monitoring breathing because the environmental noise might negatively affect the accuracy of this method [2].
The nasal temperature probe containing a thermistor is also a modality to monitor breathing. The probe is used only once for hygiene reasons (cost implications) and may

interfere with the child's normal breathing [3]. The abdominal strain gauge transducer provides another technique to monitor breathing rats. The strain gauge is strapped around the patient's chest and measures the changes in thoracic or abdominal circumference during breathing [4].
In all the above approaches, the sensing device is attached to the patient, causing them discomfort and may affect their breathing pattern. In some cases, the breathing rate is monitored visually by observing the patient. This approach is subjective and can have been significantly erroneous.

The use of the thermal imaging approach to accurately monitor the respiratory rate in infants is investigated in this study. This approach is based on detecting skin temperature change of nose and upper lip due to breathing focused on eliminating the noise in images to overcome the problems of unclear imaging. In medical applications, Enhancement images were applied and are considered very necessary to improve the quality of these images [5], [6]. To enhance thermal imaging efficiency, and obtain an accurate breathing rate. Median screens were used to improve thermal imaging [12].
In tracking the respiration using thermal imagin g, segmentation of the ROI was considered an es sential task. To deal with the subject's head movements, the Alignment Technique was used between the images and then the ROI was extracted manually from them. Also, three suggested methods were used to automatically extract the ROI then Applying feature extraction to extract the respiration signal finally, the respiration rate was extracted from the respiration signal.

2. METHODOLOGY

An advanced thermal camera (FLIR A40) that has a thermal sensitivity of 0.08° Kelvin was used for the study. The camera was fixed on a tripod in front of the patent at a distance of about one meter. The camera settings were: emissivity 0.92°, reflected temperature 15°C, and relative humidity 50%. Images were recorded at 50 frames per second. This produced 6000 thermal images over the two-minute duration (i.e. 120 seconds x 50 images). The recorded images were processed off-line using the Matlab image processing toolbox. The respiration "region of interest" (ROI) tracking method described by Al Khalidi et al. [7] was used and refined to accommodate head movement during recording.

The suggested method for monitoring breathing comprises for several steps as shown below
1. Converting the recorded thermal videos into separate images.
2. Filtering the thermal images to reduce obscuring noise.
3. Segmenting the region of interest (ROI) from the rest of the image.
4. Applying feature extraction to extract the respiration signal.
5. Processing the respiration signal to determine the respiration rate.
A median lowpass filter of size five was used to reduce unwanted noise A median lowpass filter of size five was used to reduce unwanted noise,

2.1 Manual Segmentation of the ROI

Initially, several thermal videos were recorded with subjects not making any head movements. The ROI was manually identified in the first image and was highlighted by a rectangle. The same region was then automatically extracted from the remaining images of the video.
This manual technique was effective when dealing with cases in which there were no significant head movements by the subject, as head movements caused misalignment of the selected region.
To deal with image misalignment caused by small head movements, an image registration (alignment) technique was applied. This technique was effective in correcting the differences in the location of the ROI in successive images due to head movements.
Through many iterations, it produced an optimal affine transformation [13; 14] which made the alignment of images as close as possible by considering the maximum correlations.
The alignment process was applied to all images in the video recording using the reference image (the first image in the video), and then the correlation technique was applied to measure the similarity between the alignment images[15].

Figs 1, and 2 show examples of this alignment for different types of head movements. The correlation values between the alignment images and the reference images were calculated as 0.61, and 7.02 respectively

Journal of Theoretical and Applied Information Technology
30th April 2021. Vol.99. No 8

ISSN: 1992-8645 www.jatit.org E-ISSN: 1817-3195

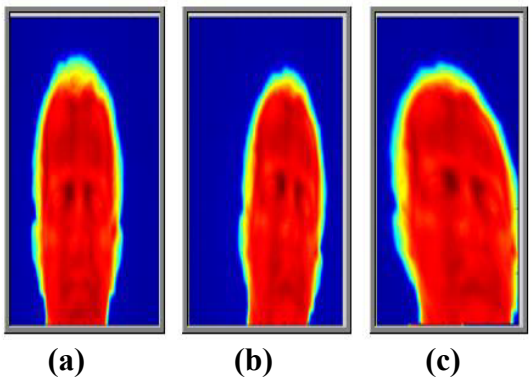

Figure 1: Alignment of two images (a) The reference image, (b) The image to be aligned with the reference image, (c) The aligned image (correlation value =0.61

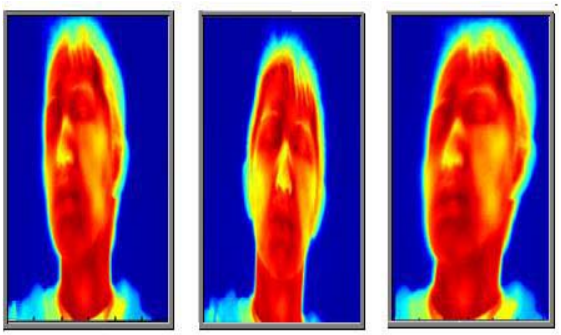

Figure. 3: Alignment of two images (a) The reference image, (b) The image to be aligned with the reference image (c) The aligned image (correlation value =0.82).

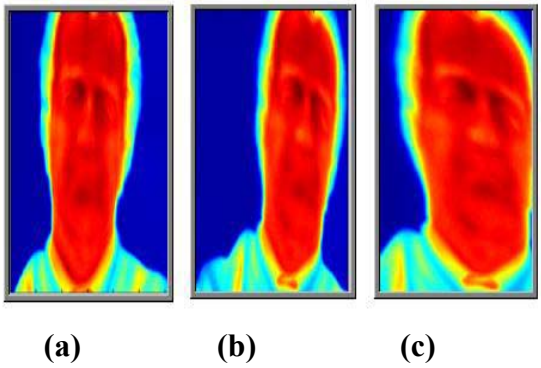

Figure 2: Alignment of two images (a) The reference image, (b) The image to be aligned with the reference image (c) The aligned image (correlation value=0.72)

As shown in these figures, the alignment technique managed to align the images and the effectiveness of the operation was quantified by calculating the correlation technique.

In some cases, despite a large correlation value, the alignment of the images and the reference image was not successful because the subject's head in the reference image was not centered on the image, the effect of which was to corrupt the correct images (see Figure .3 for an example). Also, this technique was very time-consuming; therefore it is inefficient for processing 6000 images. Besides, this technique could not deal with large head movements

2.2 Automatic Segmentation of the ROI

Automatic segmentation of the ROI from the images was based on first identifying the region and then tracking it. The method was developed for this purpose. In this method, the identification of the ROI required determining the salient features of the human face physiology, consisting of the warmest and coolest regions.

After enhanced the thermal images with a median filter, **Three methods were suggested to extract the ROI**

2.2.1 First Method to track the ROI

Initially, the subject's boundary in the image was determined using the Sobel operator [10] The Sobel edge detection scheme [11] was used to identify the boundary of the subjects' heads in the enhanced images. The Sobel masks were:

Row Mask ***Column Mask***

$$G_x = \begin{bmatrix} -1 & -1 & -1 \\ 0 & 0 & 0 \\ 1 & 1 & 1 \end{bmatrix}, \quad G_y = \begin{bmatrix} -1 & 0 & 1 \\ -1 & 0 & 1 \\ -1 & 0 & 1 \end{bmatrix}$$

The vertical highest (*Xmax*) and lowest (*Xmin*) and the horizontal highest (*Ymax*) and lowest

(*Ymin*) pixel locations of the detected edges were determined.
The center (X_0, Y_0) was identified as the center region.
The *Xmax*, *Xmin*, and the *Ymax*, *Ymin*, and represent the outermost pixels in the *X* and the *Y* directions respectively.
The circle radius (*R)* was calculated using Equ 1

$$R = Y_0 - Ymin \quad (1)$$

This enables the face to be enclosed in a circle with a radius R

The coldest temperature region in the circle was identified. Practically, the corresponding location of this region represents the tip of the nose. A second circle was placed around the identified tip of the nose; the radius of this circle was 1/16th of the number of image rows. This circle represented the ROI and was used to obtain the breathing rate. This method was successful to track the ROI for the recording images with no significant head movements.
The first tracking method worked well in cases in which there were no significant head movements. It failed when there were significant head movements

2.2.2 *The second Method to track the ROI*

After enhanced the thermal images with a median filter, The Sobel edge detection scheme was used to identify the boundary of the subjects' heads in the thresholded images [15].

The hottest area from the portion of the image that had been segmented from its background was determined. This part signified one of the two parts among the bond on the nose and the internal of the eyes. This part remained clear and labeled as the first region. The method was recurring to identify the next warmest facial area commencing the portion of the image that had remained segmented from its background. From the region of the image segmented from its background under the warmest areas, the lowest average facial temperature was found. This was representing the tip of the nose.

2.2.3 *The third Method to track the ROI*

The modification has been investigated to comply with the constraint of the previous methods.
The threshold techniques will be applied to the discrete human head from the presence background after the median low-pass filter has enhanced the thermal image and eliminated the noise. This procedure was conducted by considering the distribution of the facial temperature. The background picture temperature was comparatively lower than that of the head temperature of the subject. 30 °C was an acceptable threshold [15].
The Sobel edge detection filter was used to classify the border of the topics' heads in the thresholded images. To choose the image part enclosed by the focus's face, the advanced software mechanically overlaid on the filtered images. The setting and size of the ellipse were determined as follows

- ✓ The highest (X*max*) and lowest (X*min*) head boundary pixel positions in the vertical direction have been established and the middle among these two settings (*X*0) has been calculated.
- ✓ Positioned at *X*0, the head border points in the straight track were acknowledged, provided that *Ymin* and *Ymax*. Then, the midpoint (*Y*0) amongst *Ymin* and *Ymax* was calculated.
- ✓ The ellipse diagonals (i.e. 2a and 2b) which signify the semi-major and the semi-minor axis correspondingly were determined, where *a* and *b* were measured from *X0*, and *Y0* to *Xmin* and *Ymin* individually.
- ✓ In the meanwhile, by using the ellipse E quation 2, the position of the ellipse on t he
filtered images was then resolved to mat ch an ellipse to the image drawn by its b oundaries [9].

$$\frac{(X_i - X_0)^2}{a^2} + \frac{(Y_i - Y_0)^2}{b^2} = 1 \quad (2)$$

As seen in Figure 4, this operation retained the elliptical area containing the human face and se gments it from the rest of the image.

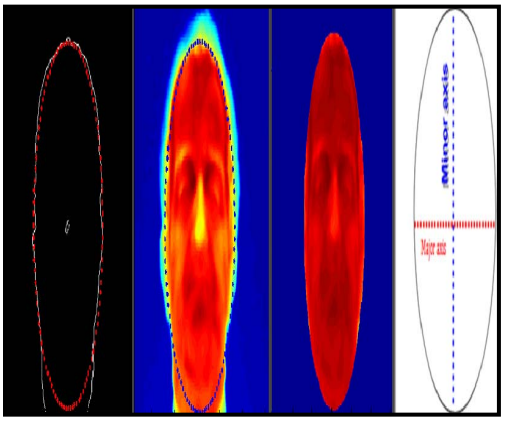

Figure. 4: The location of the ellipse over the current image which has already been filtered

The imaging spectrum covering the ellipse was primarily skimmed to distinguish the hottest and coolest area This was to assist with the choosing of the portion most influenced by nose breathing, particularly when there were significant head movements Between the bridge of the nose and the interior of an eye, a small portion corresponding to the warmest region in the human face while the coolest region was a close position to the tip of the nose. In such a way that it enclosed the tip of the nose and upper lip, a circle was put on the identified coolest area. The reason for first classifying the warmest area, then the coldest area beneath, was to reduce the likelihood of selecting an incorrect area, particularly when there were massive head movements.

This method worked well when the subject breathed through the nose (not mouth) and the mouth remained closed. The warmest facial area was an open mouth, allowing the technique to malfunction in some images because the algorithm only operates while the mouth is closed. Therefore, this problem (opened mouth) was dealt with by only looking for the warmest region on the upper part of the ellipse thus excluding the mouth region. The scanning was performed beneath the identified warmest area and the coldest area was located. The lowest value within this region was identified. This corresponded to the tip of the nose. The circle was centered on the tip of the nose, as shown in Figure 5.

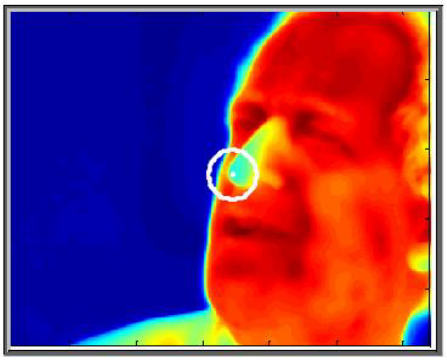

Figure. 5: The circle's location was focused on the tip of the nose.

For obtaining the respiratory signal, the circled region indicates the ROI. As seen in Figure 6, this area was first split into eight equivalent concentric segments.

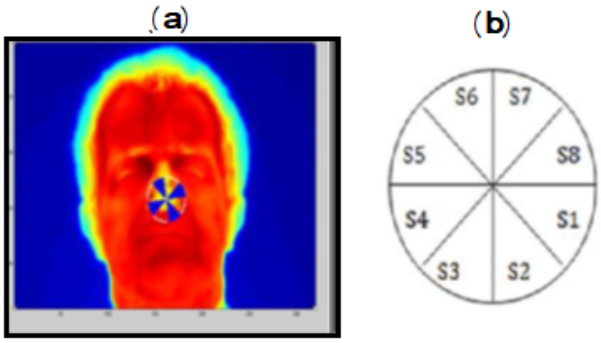

Figure.6: The ROI: (a) the ROI location at the tip of the nose, (b) the eight ROI segments

This permitted a more thorough study of temperature. In order to achieve a single value representing the segment, the pixel values for that segment were averaged. For each of the 6000 images from each subject registered, the procedure was replicated.

The averaged pixel standards of the eight segments were then distinctly strategized counter to time to produce eight respiratory indications. In demand to define the respiration rate mechanically, the respiration indications were numerically filtered using a 5th-order Butterworth filter with a cut-off rate of 1 Hz.

This cutoff rate was satisfactorily low for the respiration indication to be leveled for further handling. It was adequately high to allow 60 cycles per minute to be sensed. The time intermission of each respiration cycle (T seconds) was resolute by the software. The respiration rate (in cycles per minute) was then resolute by primary creating. Regular respiration cycles. Then, the common of this assessment was multiplied by 60 to acquire respiration amount in cycles per minute. This procedure is shown in Figure 7.

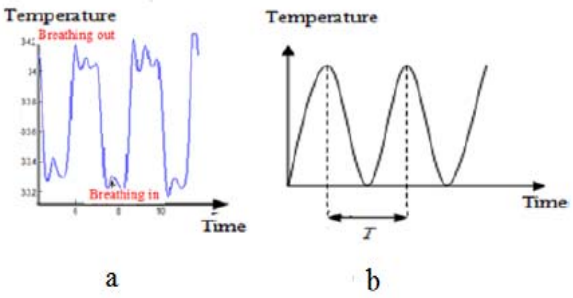

Figure 7: The breathing signal. (a) The changes directly after the change in the signal frequency are aligned with the trend of the various periods of respiration. (b) A filtered signal to suggest respiration (T).

Through measuring the correlation coefficient, the correlation between the thermal imaging method and one of the typical respiratory monitoring methods was obtained (r2).

3. RESULTS AND DISCUSSION

Of the 23 kids involved in the study 19 breathed through the nose and the leftover 4 breathed through the mouth. As the algorithm defined in this paper mechanically detects the nasal part as well as effort well when kids breathed through the mouth. The average age was 6.5 years (range 6 months-17 years). The association between thermal imaging and the typical approaches was r2 = 0.994.

An evaluation of the three methods of monitoring is given in Table 1. The table reveals that the third method provided more precise results for detecting the ROI

It visually calculated the number of images that the ROI had not successfully tracked. The performance of the monitoring techniques has been measured by determining the percentages of images that had not effectively tracked the ROI.

Table 1: Results Of Tracking Study For Different Head Movements

Subject	Number Of images	% Failure (method one)	% Failure (method two)	% Failure (method three)	Video type
SO1	6000	28	2.63	0	Random movements
SO2	6004	17.4	4.98	0	Random movements
SO3	6000	35	5.35	0.08	Random movements
SO4	5991	1.67	0	0	Regular movements
SO5	5995	0	0	0	Regular movements
SO6	6000	21.3	0.69	0	Random movements
SO7	6010	15.8	0.2	0.02	Random movements
SO8	5999	2.2	0	0	Regular movements
SO9	6000	49	0.16	0	Random movements
SO10	6010	42	1.73	0	Random movements
SO11	5999	0.16	0	0	Regular movements
SO12	1148	4.6	0.17	0	Random movements
SO13	1150	6.7	0.53	0.17	Random movements
SO14	1150	0.6	0.13	0	Random movements
SO15	2580	0.34	0.19	0.03	Regular movements
SO16	550	6.7	2	0	Random movements
SO17	50	14	4	0	Random movements
SO18	50	8	8.0	4	Random movements
SO20	39	15	0	0	Random movements
SO22	28	0	0	0	Regular movements
SO23	35	51	11.4	0	Random movements

When the ROI for an image was not correctly found, the monitoring was labeled an error and considered a failure. The proportion of tracking failure was calculated as the total number of failures divided by the total number of images in a recorded video. . Failed tracing was triggered either by the subjects stretching too far from the picture in the ROI or by the body temperature influence of the area.

4. CONCLUSION

Several methods were suggested to track the ROI in the thermal human face. In the manual segmentation method, the alignment technique was suggested to align the sequences of the thermal images with the reference one then the correlation technique was calculated between the alignment images, the ROI was detected manually in these images. In some cases, despite a large correlation value, the alignment of the images and the reference image was not successful because the subject's head in the reference image was not centered on the image, the effect of which was to corrupt the correct images, also this technique was very time-consuming; therefore it is inefficient for processing 6000 images. In addition, this technique could not deal with large head movements. For these reasons, three methods were suggested to automatically track the ROI. The results show that the third one robustly dealt withstanding, steady, and random head activities, throughout footages beneath unalike head movement categories it was likely to positively notice the ROI related with the respiration progression.

ACKNOWLEDGMENTS

The authors would like to thank Mustansiriyah University (www.uomustansiriyah.edu.iq), Baghdad-Iraq for its support in the present work

REFERENCES

[1] Moody, G.B., Mark, R.G., Bump, M.A., Weinstein, J.S., Berman, A.D., Mietus, J.E. and Goldberger, A.L.," Clinical validation of ECG-derived respiration (EDR) technique", *Computers in Cardiology*, **Vol**. 13, pp. 507-510.

[2] Baxes A. Gregory, "Digital Image processing Principles and Application" , 1994, printed in the United States of America.

[3] Storck, K., Karlsson, M., Ask, P. and Loyed, D., "Heat transfer evaluation of the nasal thermistor technique", *IEEE Transactions on Biomedical Engineering*, (1996**),Vol**. 43, no. 12, pp. 1187-1191.

[4] Nepal, K., Biegeleisen, E., and Ning, T. , "Apnea detection and respiration rate estimation through parametric modeling", *Proceedings of the 28th IEEE Annual Northeast Bioengineering Conference, Philadelphia, Pennsylvania*,(2002).

[5] Linh D. T., Linh Q.H., "Medical Image Processing in Matlab ", *The Department of Biomedical Engineering- Faculty of Applied Science HCMC University of Technology, Vietnam*, 2004.

[6] Hashim H., Jailani R., Nasir M., "A Visual Record of Medical Skin Disease Imaging using Matlab tools", *IEEE the Department of Biomedical Engineering-Faculty of Electrical Engineering University, MARA*, (2002).

[7] Farah Al-khalidi, Reza Saatchi, Heather Elphick, Derek Burke, "Respiratory Rate Measurement in Children Using a Thermal Imaging Camera", *Scientific and Engineering Research***, Vol. 6**, (2015), Issue 4 pp 1748-1756.

[8] Werthammer J., Krasner J., DiBenedetto J., Stark R. A., "Apnea Monitoring by Acoustic Detection of Airflow ", *From the Department of Pediatrics, Harvard Medical School and Brigham and Women's Hospital, Boston*, **Vol.71**, 1983, pp.53-55.

[9] Vongkornvoravej P., Roongruangsorakarn S., chaisaowong K., , "Segmentation of medical images from computerized tomography to create a 3-Dimential model of a human skull" , From the *Department computer information science, faculty of applied science*. 2004

[10] Reza S., Farah . Q., D Burke, H Elphick, " Thermal image analysis of the skin surface centred on the tip of the nose for respiration monitoring", *IEEE organised International Conference on Electronic Design and Signal* Processing, Manipal, India, 2009 .

[11] Gonzales C.R., Woods E.R., Eddins L.S., Digital Image processing using MATLAB, 2004, printed in the United States of America.

ISSN: 1992-8645 www.jatit.org E-ISSN: 1817-3195

[12] Goshtasby A.A., "2-D AND 3-D IMAGE REGISTRATION", Printed in the United States of America, 2005.

[13] Semmlow L. J., , Biosignal and Biomedical Image Processing: MATLAB –Based Applications, Printed in the United States of America. (2004)

[14] Samira A. , Farah Q.," EYES DETECTION IN THE HUMAN FACE ", International Journal of Civil Engineering and Technology (IJCIET) Vol. 9, (2018), No. 10 ,PP 1001–1007

[15] Zastaitova B., Flusser J., 2003, " Image Registration Methods: a Survey ", image and vision computing 21 (2003), pp. 977-1000.

[16] Farah Al-khalidi, Reza Saatchi, Heather Elphick, Derek Burke, , "Tracing the Region of Interest in Thermal Human Face for Respiration Monitoring" *International Journal of Computer Applications* Vol. 119, (2015), Issue 4 Publisher: Foundation of Computer Science